

# Validation of Sinus Filter Choke Temperature Model

Jan Kořinek

Jan Perner Transport Faculty, University of Pardubice, Czech Republic, e-mail: [korinek.j@gmail.com](mailto:korinek.j@gmail.com)

**Abstract** — This article discusses the relationship between the losses of a sinus filter choke. Its influence on the loaded sinus filter temperature field distribution within and on the surface, verification of these performance and temperature relationships. It includes three-dimensional transient finite element analysis (FEA) of the sinus filter choke temperature conditions based on a mathematical description of the conduction, free convection and losses and describing temperature field validation methodology. In addition, there is shown mutual evaluation of the validation measurement and FEA simulation. Finally, there are outlined further options for the future optimisation of the sinus filter choke thermal simulation.

**Keywords** — choke, sinus filter, Ansys, heat transfer, FEA, magnetism, free convection

## I. INTRODUCTION

The sinus filter is used for ensuring the device electromagnetic compatibility. For a description of heat transfer relations in magnetic field and in winding it was created 3D thermal model of the sinus filter choke.

In case of the wound parts design, magnetic circuit is influenced by thickness of the used material and high frequency part of the current, which contains wide spectrum of harmonics. In calculation it is necessary to count with basics harmonics and determine their values with consideration of other harmonic losses. Next factor is achieved for warming of the device. This warming causes rising of the sinus filter losses [1].

From the convectional heat transfer point of view, it is critical to determine as close as possible the heat transfer coefficient – see (1) in chapter III. Calculation of the heat transfer coefficient is dependent on character of the fluid flow, which is close to the sinus filter walls. It is also dependent on whole geometry of the sinus filter. For discussed simulation was calculated 13 heat transfer coefficients as boundary conditions in range from 5 to 30  $\text{Wm}^{-2}\text{K}^{-1}$ . These values were constantly modified during simulation with temperature influence. In flow for actual fluid it is then necessary to consider kinematic and dynamic viscosity, heat conductivity, volume expansion and also specific heat capacities.

From reasons above, it was realized an experimental measurement for validation of losses and for validation of the FEA simulation of the temperature distribution through the sinus filter choke. It was also measured current, which goes through the sinus filter. Thanks to that, it is possible to divide losses in part of the core and part of the winding. Values from these parts are used as boundary conditions for the FEA simulation of the temperature distribution. Measurement of achieved

temperature values on a physical sample of the sinus filter is then used for overall comparison with the FEA simulation.

## II. WIRING DESCRIPTION OF SINUS FILTER

Sinus filter is designed for nominal current 16 A, switching frequency from 2 kHz and for short-time overload 1.5 times. Output voltage is from 0 to 500 V. Supply wire from a low voltage net 3x230/400V was connected into the three phases commutating choke. Commutating choke was plugged into the frequency converter and on the output clamps the sinus filter was connected. Measurement were carried out on the sinus filter however, simulation was performed for the geometry of the sinus filter choke. Behind the sinus filter, a constant load was plugged in. Sinus filter input was connected to the output inverter of the frequency converter Siemens Masterdrives of the power 11 kW. Frequency converter built on his output an associated pulse width modulation voltage PWM pulsing with 4 kHz frequency. Sinus filter output was connected to the electric motor. This voltage was filtrated with the bottom gate LC type under the 1 kHz limit. Behind this bottom gate (sinus filter), the voltage was brought the constant load.

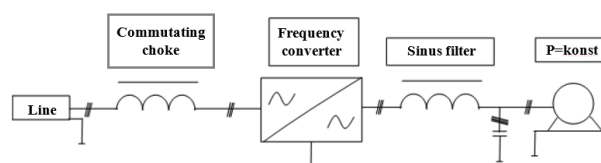


Fig. 1. Schematic wiring description of sinus filter.

## III. SINUS FILTER IMPLEMENTATION METHODIC USING FINAL ELEMENT METHOD MODEL

For a calculation of the temperature field distribution the sinus filter choke model with characteristic dimensions based on product specification was created. Computation task, its settings, mesh creation, definition of boundary conditions and final post processing were conducted with the Ansys Transient Thermal software. Simulation considers transient case, therefore the temperature change process can be observed in core, winding frame, windings and the clamping construction.

1) *Geometry and materials of the model:* The filter core consists of isotropic cold rolled metal sheets. Their count defines the final core width. Since the metal sheets are in close contact, for the calculation purposes it is considered the monolithic core model keeping the characteristic

dimensions according to Waasner DIN EN 10106, EI 175/175 with material characteristic M330-50A. To this model the material properties were assigned which are essential for a thermo-conductive calculation. These are especially the density ( $7850 \text{ kgm}^{-3}$ ) and heat conductivity ( $60.5 \text{ Wm}^{-1}\text{K}^{-1}$ ). For the calculation purposes, the similar assumption was considered as well as in the case of the copper winding. The winding represents a monolithic solid with the assigned material properties of copper according to EN 13601 Cu-ETP with density ( $8933 \text{ kgm}^{-3}$ ), heat conductivity ( $400 \text{ Wm}^{-1}\text{K}^{-1}$ ) and characteristic dimensions related to the sinus filter product specification. To the winding frame the material characteristics for *Pocan B4239* are assigned with density ( $1500 \text{ kgm}^{-3}$ ) and heat conductivity ( $0.25 \text{ Wm}^{-1}\text{K}^{-1}$ ). For the model mesh optimization, it was not considered a ribbing on the horizontal area of the frame. The L-profile of the clamping construction contains the data about the density and heat conductivity of the carbon steel. The complete 3D model is represented below in Fig. 2.

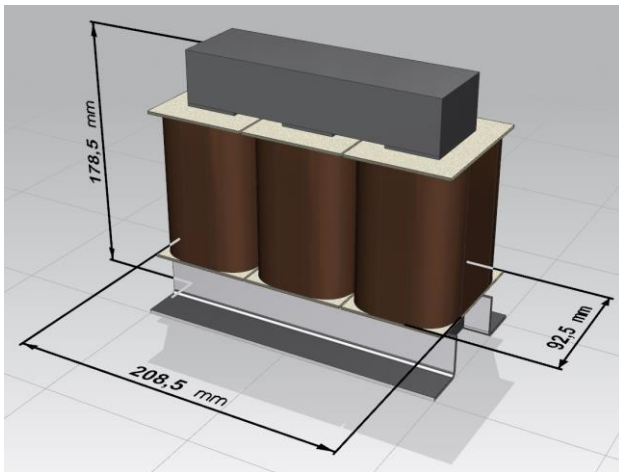


Fig. 2. 3D CAD model of sinus filter.

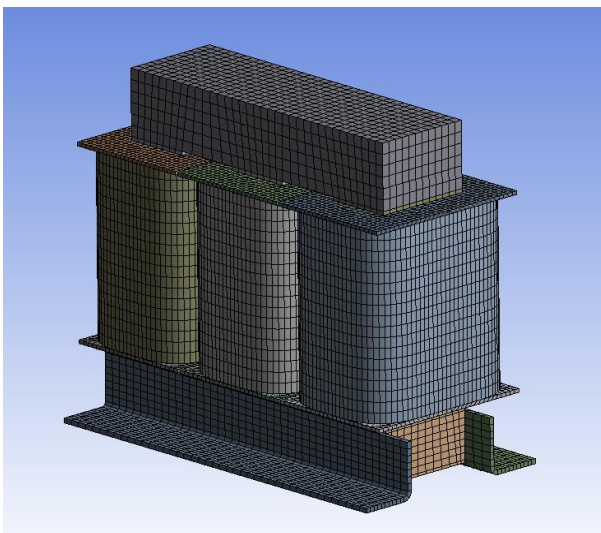


Fig. 3. Mesh of sinus filter 3D model.

2) *Mesh properties*: For reaching the lowest possible calculation time it was placed emphasis on optimization of element shapes which build the whole model mesh. The

whole model mesh is shown in Fig. 3. Approximately 85 % of the mesh consists of hexahedral type elements. The whole model is built by 53 936 elements.

3) *Initiatory and boundary conditions of the simulation*: One of parameters entering into the calculation is the initial temperature. Due to the fact that during the experimental validation the environment temperature of the air was  $15 \text{ }^\circ\text{C}$ , the same temperature was considered for the simulation. The final temperature settling time was set on 80 000 s.

Boundary condition of the heat flow was globally applied on the core and sinus filter winding. Manufacturer intention was to find out, for how long is possible to overload the sinus filter of 1.5 times of the nominal alternate current. Based on that losses on the core was  $17.2 \text{ W/winding}$ . Losses on the stand alone winding are  $15.9 \text{ W}$ . These values are crucial for heat distribution across whole geometry and has to be taken in account. Both of them were calculated and provided by manufacturer.

Boundary condition for the convective heat transfer is defined by value of the heat transfer coefficient  $h (\text{Wm}^{-2}\text{K}^{-1})$ . For calculation of all heat transfer coefficients it is considered influence of surrounding thanks to free convection mathematical relationship which is linked to the determination of heat transfer coefficient. Amount of the heat transfer into open surrounding from surface of the sinus filter choke is then expressed by heat transfer coefficient values – see chapter I. Air is considered as an ambient medium and its properties as temperature depended. In consequence of this fact we get for each determining temperature other values of Grashof, Prandtl, Rayleigh and Nusselt numbers. The resulting heat transfer coefficient where  $Nu$  is Nusselt number,  $L$  is characteristic dimension and  $k$  correspond to thermal conductivity – see (1) – which is related to certain geometrical area is thus continuously changing till reaching the established temperature [2] [3]. Due to very comprehensive problematics related to hear transfer coefficient, the detailed discussion about calculation is over the scope of the article.

$$h = Nu \cdot k / L \quad (1)$$

#### IV. VALIDATION TEMPERATURE MEASUREMENT

The sinus filter was placed in an area on the horizontal plate without forced flowing or actuation of further heat sources. Ambient temperature of air was  $15 \text{ }^\circ\text{C}$ . So the character of flow around the walls corresponds with the free convection. Sinus filter was powered by alternating current frequency of 50 Hz with superimposed high-frequency component resulting from switching frequency of the frequency converter. Temperature measurement of the sinus filter loaded with the 23 A current has taken place using thermocouples and thermovision. There could be also taken in account usage of resistance method thanks to that is possible to find out the average thaw of windings. However, in our case was used thermovision which provided to us accurate temperature field distribution and not just average value.

Thermocouple using principle of the direct temperature difference conversion in electric voltage is the class T with the maximum allowed usage temperature to  $350 \text{ }^\circ\text{C}$ . It is produced from the combination of copper and

constantan material. The measurement error is 0.75 % at the temperature above 0 °C. Thermocouples are connected with the auto-calibrating unit *National Instruments® Ni PXI*. This unit is used for digitization, archiving and for evaluation of the warming procedure. In total, it was used four thermocouples allocated at different measuring points – see Fig. 4. Based on sinus filter design and measurement possibilities, thermocouples were placed as close as possible to places with highest expected temperature without any damage of sinus filter. Thermocouple No. 1 measures the temperature on the core surface. Thermocouple No. 2 is positioned under surface between the core and winding frame (place with highest expected temperature). Thermocouple No. 3 is inserted between windings and thermocouple No. 4 is in the opposite location on the bottom side of the core parallelly with the plate on which the sinus filter is placed.

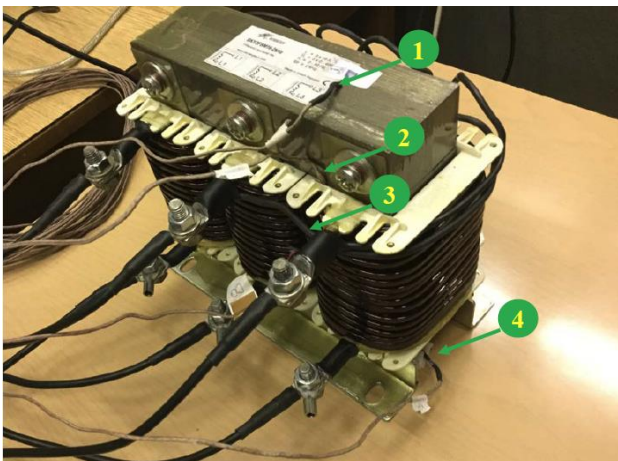


Fig. 4. Sinus filter SKY3FSM16-2kHz with thermocouples.

The second method of the temperature measurement was the screening of infrared radiation generated by the sinus filter surface. For this measurement the thermovision *Fluke® Ti125* was used. For radiated infrared spectrum volume the fundamental factor is the surface temperature and emissivity of the material surface. Based on these recorded data the surface temperature is subsequently calculated by a thermocamera. Emissivity, which was set up in the device for the detection, was calibrated on the value 0.96 based on comparison with the measurement which was performed with the second sinus filter. The temperature of the second sinus filter is the ambient temperature. The temperature range for usage of the thermovision is from -20 °C up to 350 °C with accuracy  $\pm 2$  °C or 2 % based on fact which value is the bigger one. The temperature sensitivity of the detection is 0.1 °C if the temperature of the measured object is 30 °C according [4]. For the visualisation of the recorded data the colour range with blue-red spectrum during the whole measurement was used. The reason for usage of this spectrum is better graphicness in comparison with the FEA simulation of the temperature allocation.

## V. MEASURED VALUES OF WARMING

### 1) Resulting temperatures based on Ansys simulation:

From the performed FEA simulation of the sinus filter choke it was calculated the 3D temperature distribution across inside and surface geometry which is visualized in

Fig. 5a. Colour spectrum expresses the local temperature in °C. Calculation was executed as transient with the time step 1 s in the range from 0 to 80 000 s. Stabilized situation was reached after 154 iterations in the time 70 100 s. As a criterion for stabilized solution was set up an increment of 0.001 °C. In the Fig. 5b can be also seen thermal gradient between location with highest temperature and surface of middle winding. Based on simulation, the gradient value is in this case 3,3 °C. In Fig. 6 the minimum and maximum temperature characteristics in dependency on time while the sinus filter choke is under load are shown.

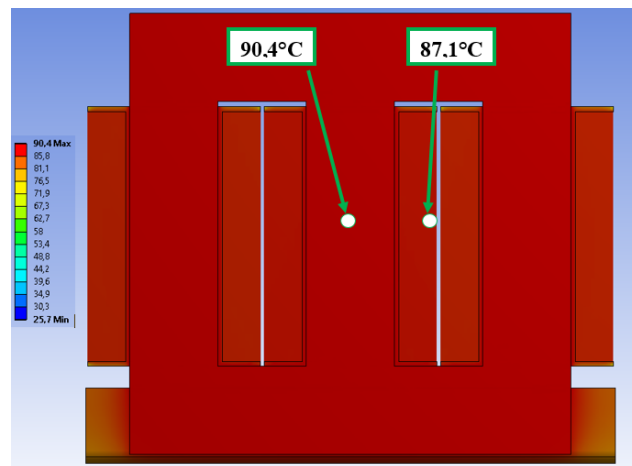
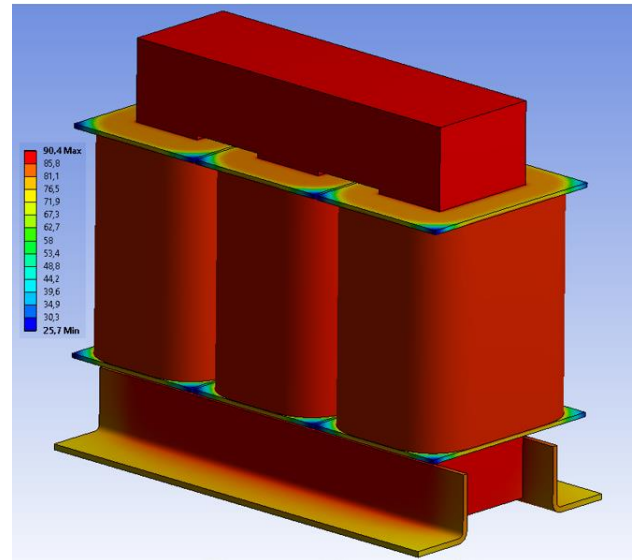


Fig. 5. a) Stabilized 3D temperature field in time of 70 100 s.  
b) Longitudinal cross-section through sinus filter choke.

It was reached the global maximum stabilised temperature at the value 90.4 °C. It is obvious that already after five hours the temperature reaches 97 % of its maximum value. The final stabilisation was reached after next 14.5 hours and temperature increase of about 2.5 °C. Visualized dependency has an exponential character. The lowest stabilised value on the whole sinus filter is 25.7 °C. This reaches 97 % of its maximum value already after 4 hours. After further 13.2 hours the stabilised temperature is reached by the increase of about 0.8 °C. Maximum temperature area occurs in the core especially at the



middle winding according to Fig. 5b. Temperatures near to maximum temperatures are also in the upper part of the core. Temperatures direct on the winding are in the range between 86 °C and 87 °C. Maximum is then reached on the middle winding. The winding frame has its temperature maximum inside in the location of the contact with the core, at the value 90.4 °C. Minimum temperature (25.7 °C) is then in the corners of the horizontal edges. This location is thus the global minimum of the global sinus filter choke.

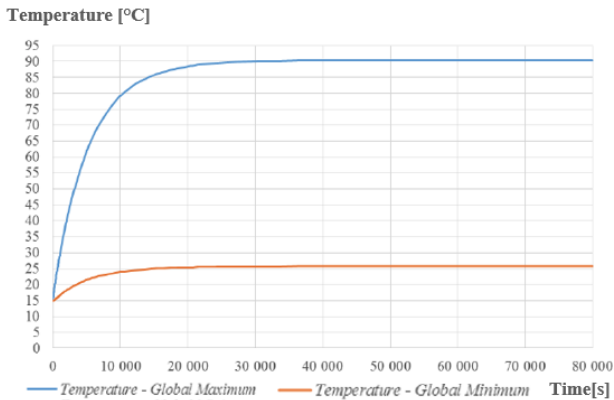


Fig. 6. Settling of maximum and minimum temperatures.

2) *Resulting temperatures based on thermocouple measurement:* From the thermocouple measurement the warming characteristic was derived. The temperature monitoring from the start of loading took 5 hours. Based on the measured data it was done the trend regression for smoothing.

For better orientation it were included the warming data from the simulation into the graph in Fig. 7 in order to enable the temperature trend comparison. Figure 7 demonstrates that the warming character from the simulation is approaching to the performed measurement.

The highest measured temperature after 5 hours was measured in the point No.2 with value 82.1 °C and thus in the location between upper part of the winding frame and core. 76.4 °C was identified on windings in the point No. 3. On the core surface in the point No. 1 it was found out 60 °C and in the point No.4 the temperature was 60.6 °C.

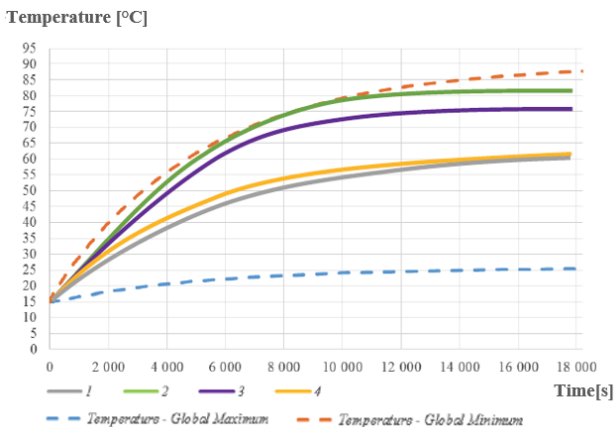


Fig. 7. Settling of temperatures from points 1–4 measured by thermocouples.

3) *Resulting temperatures from the thermovision measurement:* On the below presented figure series it is always possible to see the temperature field recorded by the thermovision with the visualization of the temperature range and maximum temperatures reached in the concrete view. In addition, it will be introduced the assigned view of the 3D model from the simulation for comparison. Due to the fact that the real warming characteristic was measured for 5 hours, the compared views from the simulation are used as well from this time frame and not from the period of the stabilised state, that means derived for the time 18 000 s. Nevertheless, from Fig. 7 it is visible that the difference of the maximum temperature between this time frame and the stabilised state time is minimal.

After deduction of the simulation data, the value corresponds with 2.5 °C.

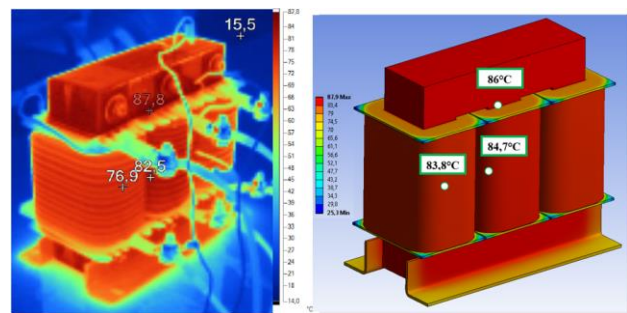


Fig. 8. Comparison of temperature fields between thermovision and simulation in time of 5 hours.

In Fig. 8 there are highlighted points for better orientation in the locations on the surface of the side and middle windings. Furthermore, there is shown the highest measured temperature in the actual snapshot at the value 87.8 °C. The same can be seen in the right side of the figure. It is visible that the differences here are commonly reaching 2.5 °C except the side winding where the temperature difference is up to 6.9 °C. From snapshots it can be derived that the real temperature field allocation on the middle winding corresponds with the simulation.

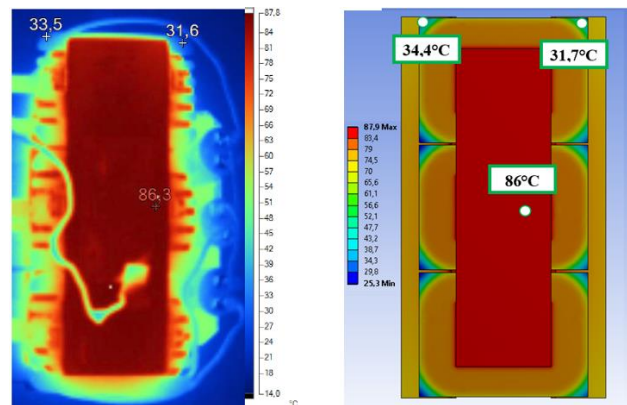


Fig. 9. Comparison of temperature fields between thermovision and simulation in time of 5 hours – top view.

In the locations at the winding frame edges the lowest temperature after stabilisation based on the simulation was determined. Verification is visible in Fig. 9. The measured temperatures in these edges were 31.6 °C and

33.5 °C. Highest difference against the simulation was in this case 1 °C. From the temperature allocation of the winding frame point of view, the calculation model corresponds in these locations with the reality. In Fig. 10 in the bottom area the measured temperature of the core near to the plate surface is visible. Compared to 85.6 °C from the simulation the measured temperature here is 83.4 °C. The temperature in the upper part from the core side differs not so much, only up to 1.1 °C. It was measured here 87.6 °C compared to 86.6 °C from the simulation.

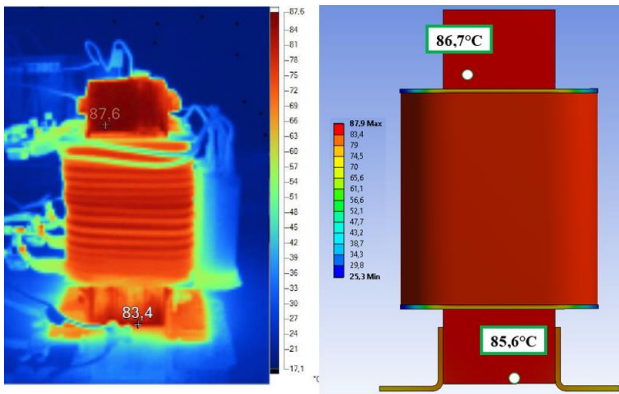


Fig. 10. Comparison of temperature fields between thermovision and simulation in time of 5 hours – side view.

In Fig. 11 the temperatures from measurement points 1–4 are listed. Maximum reached temperatures in these points are measured or calculated in the timestamp of 5 hours operation under load. The simulations are derived from the same locations with help of virtual probes. In case of infrared radiation, which was recorded by thermovision, the temperatures of the measurement locations are derived in figures with support of software for analysis and recording of the infrared figurers.

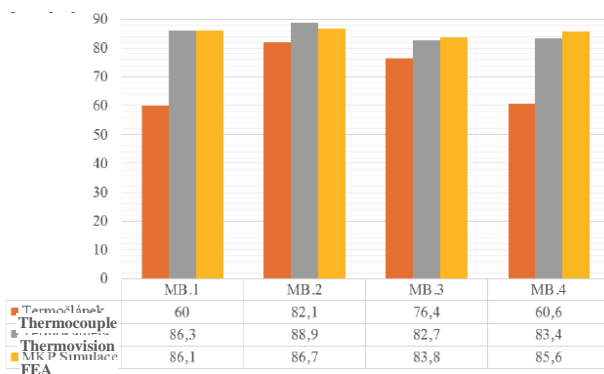


Fig. 11. Comparison of maximum temperatures by thermocouples, thermovision and FEA simulation.

## VI. CONCLUSION AND POTENTIAL FURTHER OPTIMIZATION

Based on comparison of the above mentioned methods, the FEA simulation seems to be the most pessimistic one from the reached maximum point of view. It is possible to say that its results are most approaching in all measuring points to the values which were measured by the thermovision. A considerable difference of temperatures measured by the thermocouple appear in points 1 and 4,

and thus on the upper and bottom horizontal sides of the core frame. Potential explanation could be found in the way of the thermocouple fixture, whose contact with the core surface may not be ideal. In general, the thermocouples seem to be the most optimistic solution from the reached temperature measurement point of view. To this statement contributes the fact that the thermocouple itself has its own level of the thermal conductivity. In the contact place thus comes to the heat transfer from the sinus filter material into the thermocouple. Therefore, the lower temperature is measured than the temperature, which is really on the sinus filter surface and its surrounding. As can be seen in Fig. 11 agreement between simulation and thermovision is satisfactory, therefore assumption of thermal gradient agreement is taken in account. Considering of surrounding temperature of 40°C in closed enviroment, sinus filter would be probably thermally overloaded in this case. Here is necessary to remind that main focus of the article is not sinus filter dimensioning for a specific application but to acquire data for validation of FEA simulation.

By the comparison of both thermovision and sinus filter choke 3D model views it is obvious that in some locations the temperature field differs more from the real allocation. This can be observed both in the location of the contact between the base plate with the clamping construction beam and by the winding nearby the fastening contacts for the supply and as well on the horizontal area of the winding frames. In order to improve the accuracy of the temperature allocation this could be optimized in the simulation through the improvement of the 3D geometry precision into higher details, e.g. implementation of winding frame ribbing, fastening contacts, base plate geometry and condenser holders.

The temperature field allocation on all windings corresponds with its character to reality, nevertheless the temperature difference between the middle and side windings are in the reality higher than they were calculated by the simulation. This can be explained by the influence of the precision grade of the winding in the 3D model. The smooth surface was considered here for the calculation simplification. At the real product of the sinus filter the surface is due to the wire winding grooved. This fact has an influence on the flowing during free convention, when its character is changed due to the radial direction of the current through the winding grooves. The effect is a change of the heat transfer coefficient and thus the change of the resulting surface temperature. Implementation of more detailed winding geometry into the 3D model leads to the usage of correlation relationships, modified for the shape of the concrete geometry. Further, the losses allocation in the winding has influence on the temperature differences in the single windings. In the 3D model in the boundary conditions the same losses in every winding are considered. In the reality, the losses can be slightly different on the single windings. This would have the effect on the temperature difference increase between single windings as the results.

The above mentioned facts show the new potential which can be used for further concretization of the input parameters for the mathematical simulation model. In the near future more geometrical details can thus be implemented into the actual model, application of the values of measured losses and thus reaching the change of the temperature field allocation.

## ACKNOWLEDGMENT

This text was created with support of the project Studentská grantová soutěž SGSDJFJ\_2016001. Creation was also supported by company SKÝBERGTECH s.r.o. which borrowed sinus filter and provided consultations during validation measurements.

## REFERENCES

- [1] KRISHNAMOORTHY P. Electromagnetic and Heat Transfer Modeling of Microwave Heating in Domestic Ovens. Lincoln: University of Nebraska at Lincoln, May 2011.
- [2] NOŽIČKA, J. *Základy termomechaniky*. Praha: Vydavatelství ČVUT, 2001. ISBN 80-01-02409-1.
- [3] ŠESTÁK, J. a F. RIEGER. *Přenos hybnosti, tepla a hmoty*. Praha: Vydavatelství ČVUT, 1993. TA357.Š37 1993.
- [4] FLUKE. fluke.com: Ti90, Ti95, Ti100, Ti105, Ti110, Ti125 TiR105, TiR110, TiR125 Performance Series Thermal Imagers [online]. © 2012 [cit. 2016]. Available on: <http://www.fluke.com/fluke/czcs/support/manuals/default.htm>